THE JOURNAL OF PHYSICAL CHEMISTRY B

Article

pubs.acs.org/JPCB

Catalytic Electrochemistry of Xanthine Dehydrogenase

Palraj Kalimuthu,[†] Silke Leimkühler,[‡] and Paul V. Bernhardt*[,†]

[†]School of Chemistry and Molecular Biosciences, University of Queensland, Brisbane 4072, Australia

[‡]Institut für Biochemie und Biologie, Universität Potsdam, 14476 Potsdam, Germany

Supporting Information

ABSTRACT: We report the mediated electrocatalytic voltammetry of the molybdoenzyme xanthine dehydrogenase (XDH) from *Rhodobacter capsulatus* at a thiol-modified Au electrode. The 2-electron acceptor *N*-methylphenazinium methanesulfonate (phenazine methosulfate, PMS) is an effective artificial electron transfer partner for XDH instead of its native electron acceptor NAD^+. XDH catalyzes the oxidative hydroxylation of hypoxanthine to xanthine and xanthine to uric acid. Cyclic voltammetry was used to generate the active (oxidized) form of the mediator. Simulation of the catalytic voltammetry across a broad range of substrate and PMS concentrations at different sweep rates was achieved with the program DigiSim to yield a set of consistent rate and equilibrium constants that describe the catalytic system. This provides the first example of the mediated electrochemistry of a xanthine dehydrogenase (or oxidase) that is uncomplicated by interference from product oxidation. A remarkable two-step, sequential oxidation of hypoxanthine to uric acid via xanthine by XDH is observed.

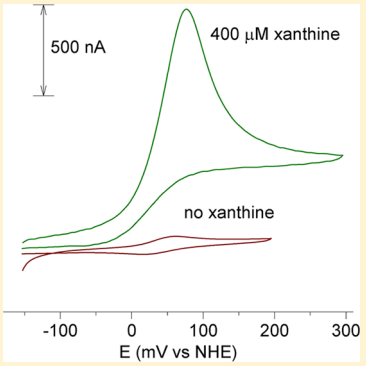

INTRODUCTION

Enzyme electrochemistry continues to provide opportunities for the design and optimization of biosensors due to the inherent selectivity and sensitivity of the enzyme and the simplicity of voltammetric analysis.[1−6] In many cases, direct heterogeneous electron transfer (between electrode and the enzyme cofactors) is prevented by exceedingly large distances and improper orientation of the adsorbed enzyme.[7−9] To resolve this problem, small molecular weight mediators may be used as shuttles between the enzyme cofactors and the electrode.[10−12] The mediators may be either aromatic organic compounds (quinones, aromatic amines, and heterocycles) or transition metal complexes.[13] An ideal mediator should be characterized by high stability in both its oxidized and reduced forms and facile heterogeneous electron transfer.

Xanthine dehydrogenase (XDH) is a complex molybdenum−iron−sulfur−flavoprotein found commonly in bacteria and animals. It is by far the most intensively studied mononuclear Mo enzyme and is one of only four Mo enzymes found in humans. XDH catalyzes the hydroxylation of purines, pyrimidines, pterins, and aldehyde substrates using NAD^+ as its electron acceptor.[14−16] XDH and the closely related xanthine oxidase (XO), which is able to donate electrons to molecular oxygen, are both involved in several medical conditions including xanthinuria (excess xanthine), gout (excess uric acid), ischemia-reperfusion, hepatitis, cancer, and inflammatory disorders.[17] All XDH/XO enzymes contain a Mo active site comprising a single bidentate coordinated pyranopterin-dithiolene ligand (molybdopterin), an equatorial sulfido, axial oxido, and an equatorial hydroxido/aqua ligand depending on pH.[18−20]

Like other oxidase enzymes, H_2O_2 and O_2^- are products of XO activity when dioxygen is reduced.[21] The electroactivity of H_2O_2 provides a method for monitoring XO turnover electrochemically while not requiring electron transfer with the enzyme. By contrast, XDH exhibits very low oxidase activity and preferentially uses NAD^+ as an electron acceptor,[22] which is electrochemically inert so alternative approaches are required to provide a means of monitoring and maintaining catalysis.

In recent years, we have demonstrated both mediated[23−26] and direct[27−30] catalytic electrochemistry with a variety of molybdoenzymes.[2] Our studies with the bacterial *Rhodobacter capsulatus* XDH[31,32] and bovine XO[33] in the absence of a mediator have revealed very complicated electrochemical behavior. We have shown that electron transfer between the electrode and XDH is mediated by the *product* of XDH turnover (uric acid in its 2-electron oxidized imine form, Figure 1), which acts as a nonphysiological electron acceptor in place of NAD^+.[32] As uric acid is the product of xanthine oxidation (Scheme 1), the mechanism is autocatalytic and complex.[32] The natural substrates of XDH, hypoxanthine and xanthine, are also electrochemically active but undergo coupled 2-electron, 2-proton oxidations at much higher potentials (Figure 1).[34−36]

There are only a few examples of mediated XO (bovine) electrochemistry in the literature, and all of these have employed mediators that have redox potentials in the same region as the uric acid/uric acid imine couple, i.e., ferrocene complexes and the ferricyanide derivative Prussian blue.[37,38] In light of our recent findings,[32] concurrent oxidation of uric acid at the same potentials of the mediators would have been unavoidable in these reports as well.[37,38] Herein, we report the clean mediated electrocatalysis of *R. capsulatus* XDH using the

Received: July 25, 2012
Revised: August 29, 2012
Published: August 30, 2012

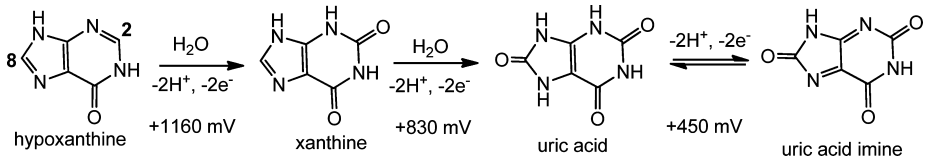

Figure 1. Redox reactions and redox potentials of purines relevant to this work (mV vs NHE at pH 8). Relevant C-atom numbering shown for hypoxanthine.

Scheme 1

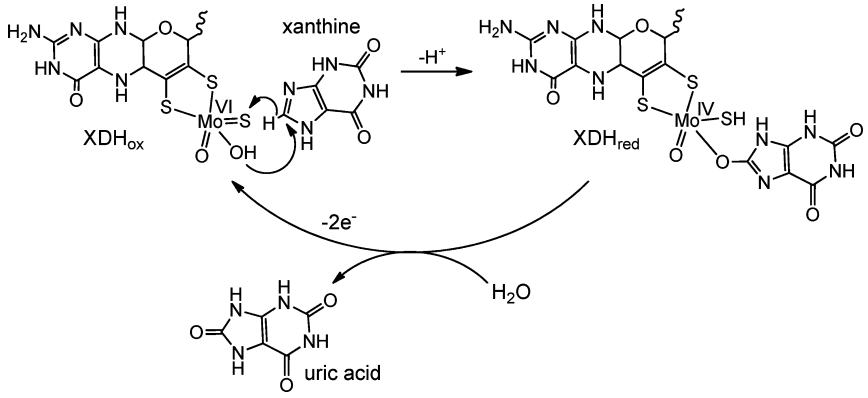

electron acceptor *N*-methylphenazinium methanesulfonate (phenazine methosulfate, PMS, Figure 2). PMS undergoes a

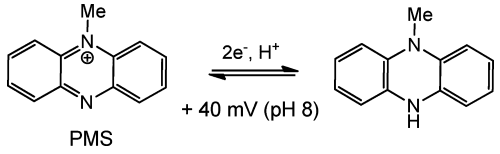

Figure 2. Structures of the oxidized and reduced forms of PMS (pH 8, potential vs NHE).

reversible two electron redox reaction at a potential well below uric acid; thus, interference from product oxidation is avoided. This is the first time that true mediated electrocatalysis of a xanthine oxidoreductase has been demonstrated without any interference from product oxidation.

The other objective of this study is to analyze the enzymatic kinetics via simulation of the catalytic voltammetry. It is indeed possible to relate the catalytic voltammetric responses to characteristic enzyme dependent rate constants (Michaelis–Menten kinetics) and enzyme-mediator (outer sphere) electron transfer kinetics.

EXPERIMENTAL SECTION

Materials. *Rhodobacter capsulatus* xanthine dehydrogenase was purified from a heterogeneous expression system in *E. coli* as previously described.[20] Xanthine, hypoxanthine, and phenazine methosulfate were purchased from Aldrich and were used as received. All other reagents used were of analytical grade purity and used without any further purification. All solutions were prepared in purified water (Millipore, resistivity 18.2 MΩ·cm). Tris (acetate) buffer (50 mM) was used for experiments at pH 8.

Electrochemical Measurements and Electrode Cleaning. Cyclic voltammetry (CV) was carried out with a BAS 100B/W electrochemical workstation. A gold working electrode was first cleaned according to a published protocol[39] then modified with 5-(4′-pyridinyl)-1,3,4-oxadiazole-2-thiol (HPyt) as described.[40] A platinum wire counter electrode and Ag/AgCl reference electrode were used (+196 mV vs the normal hydrogen electrode, NHE). Potentials are cited versus NHE. Experiments were carried out in argon purged solutions.

Enzyme Electrode Preparation. A 3 μL droplet of XDH (66 μM) in 50 mM Tris buffer (pH 8.0) was pipetted onto the conducting surface of an inverted, freshly prepared Au-HPyt working electrode, and this was allowed to dry to a film at 4 °C. To prevent protein loss, the electrode surface was carefully covered with a perm-selective dialysis membrane, presoaked in water. The dialysis membrane was pressed onto the electrode with a Teflon cap and fastened to the electrode with a rubber O-ring to prevent leakage of the internal membrane solution. The resulting modified electrode was stored at 4 °C in 50 mM Tris buffer solution (pH 8.0) when not in use. The enzyme was confined to a thin layer beneath the membrane, while substrate and mediator were able to diffuse across the membrane.

Electrochemical Simulation. The DigiSim (version 3.03b) program was employed to simulate the experimental cyclic voltammograms.[41] The experimental parameters restrained in each case were the working electrode surface area (0.053 cm^2), determined from variable sweep rate cyclic voltammetry of hydroxymethylferrocene (diffusion coefficient 6.7×10^{-6} cm^2 s^{-1}),[11] and the double-layer capacitance (5 μF) was determined from the voltammetry of PMS in the absence of XDH or substrate. Semi-infinite diffusion was assumed and all pre-equilibration reactions were disabled. Diffusion coefficients of 10^{-6} cm^2 s^{-1} were used for PMS (oxidized and reduced), xanthine, and uric acid. All forms of XDH (oxidized, reduced, and substrate or product bound) were taken to have equal diffusion coefficients (10^{-8} cm^2 s^{-1}). The heterogeneous rate constant (k_0) for PMS_{ox}/PMS_{red} was determined by simulation of the sweep rate dependent voltammetry (in the absence of XDH) and a value of 1.2×10^{-2} cm s^{-1} was used in all cases. The redox potential of PMS was calculated as the average of the anodic and cathodic peak potentials. All of the above-mentioned parameters were then held constant during

dx.doi.org/10.1021/jp307374z | J. Phys. Chem. B 2012, 116, 11600–11607

simulations of experiments at different sweep rates (2−50 mV s^{-1}), substrate concentrations (xanthine or hypoxanthine, 100−1600 μM), and PMS concentrations (2−5 μM). Only the homogeneous rate constants were allowed to vary ($k_1 - k_4$ and k_{-1}−k_{-4}, Scheme 2) until a single set of parameters that modeled all experiments was obtained.

Scheme 2. PMS-Mediated Electrochemically Driven Catalysis of XDH

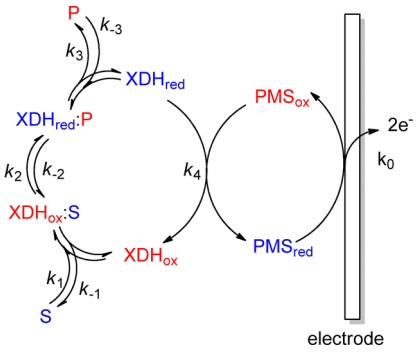

RESULTS AND DISCUSSION

Mechanism of XDH Electrocatalysis. XDH is a 275 kDa $(\alpha\beta)_2$ heterotetramer that bears four different redox active cofactors; the Mo active site, two spectroscopically distinct [2Fe2S] clusters (FeSI and FeSII), and an FAD, the site at which the native electron partner NAD^+ binds during turnover. We have assumed that XDH:xanthine reaction follows Michaelis−Menten kinetics comprising substrate binding (k_1/k_{-1}), turnover (k_2/k_{-2}), and product release (k_3/k_{-3}). All intramolecular electron transfer reactions within XDH (Mo → FeSI, FeSI → FeSII, and FeSII → FAD) were assumed to be rapid and non-rate limiting. A simplified double substrate ping-pong mechanism is employed to model the overall reaction kinetics (Scheme 2). Briefly, XDH_{ox} (the active Mo^{VI} form) reacts with substrate (S = xanthine or hypoxanthine) which binds with the enzyme (k_1) and then undergoes hydroxylation (k_2). Following product release (k_3), XDH_{red} (the inactive form) reacts with the mediator PMS_{ox} in an outer sphere 2-electron cross-reaction (k_4). It is assumed that the site of oxidation by PMS_{ox} is at the FAD cofactor (now in its reduced hydroquinone form following intramolecular electron transfer from Mo to FAD). It is known that the natural electron acceptor NAD^+ binds at the FAD site and that single turnover experiments result in two electron reduction of the FAD cofactor. The XDH_{red}:PMS_{ox} reaction is treated as a simple bimolecular outer-sphere electron transfer reaction (no pre-equilibrium). Given the large driving force of this electron transfer cross-reaction (ca. +400 mV on the basis of the PMS and FAD redox potentials),[31] the reverse reaction (k_{-4}, PMS_{red} + XDH_{ox}) is negligible. XDH is confined to a thin layer on the Au/HPyt electrode surface entrapped under a membrane (M.W. cutoff 12 kDa), whereas the substrates/products (hypoxanthine, xanthine, and uric acid) and PMS (M.W. < 200 Da) are under diffusion control and may cross the membrane.

Mediator Selection. Potentiometric redox titrations have defined the potentials of the Mo, Fe−S, and FAD cofactors, and on this basis, the enzyme is fully oxidized at potentials higher than ca. −250 mV vs NHE.[31] Uric acid, the product of XDH catalysis, is oxidized at ca. +450 mV vs NHE (pH 8) at an edge-plane pyrolytic graphite (EPG) electrode,[32] so this defines the window within which mediated XDH catalysis may be observed without interference from uric acid oxidation. We have chosen the mediator PMS (+40 mV, pH 8), which undergoes a 2-electron/1-proton reversible electron transfer reaction (Figure 2).

Xanthine As Substrate. As an example, the mediated electrocatalytic voltammetry of XDH in the presence of xanthine mediated by PMS is shown in Figure 3. In the absence of xanthine, a well-defined symmetrical $PMS_{red/ox}$ wave is observed at +40 mV vs NHE with a peak-to-peak separation of 47 mV (Figure 3, red curve), which is expected for a quasi-reversible 2-electron process. This current is governed by the diffusion of both oxidized and reduced forms of PMS. No redox responses from XDH are seen under these conditions.

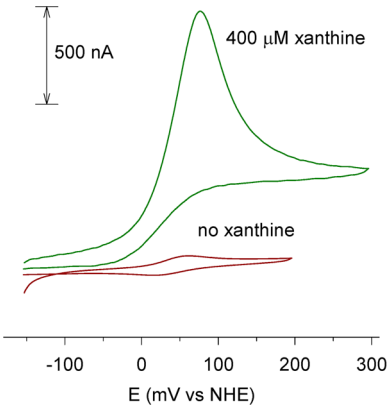

Figure 3. CVs obtained for PMS (5 μM) in the absence (red) and presence (green) of 400 μM xanthine at the Au/HPyt/XDH electrode (50 mM Tris buffer, pH 8) at a sweep rate of 5 mV s^{-1}.

Upon the addition of xanthine (400 μM) to the same cell, a dramatic amplification of current is observed, and the waveform is altered (Figure 3, green curve). On the anodic sweep, a transient waveform is observed due to diffusion layer depletion, while on the reverse cathodic sweep, the wave is sigmoidal. As will be demonstrated, the transient anodic wave is due to xanthine depletion, not PMS, within the diffusion layer. Note that no redox response from uric acid (ca. +450 mV, pH 8) is observed within this potential range.

The catalytic current is dependent upon the diffusion of PMS_{red} to the electrode surface, reaction between xanthine and XDH, and the reaction between PMS_{ox} and XDH_{red} (Scheme 2).[9] In Figure 4, the effect of xanthine concentration is shown (400−1600 μM) in the presence of a constant concentration of PMS (5 μM) and at a fixed sweep rate (10 mV s^{-1}). The voltammograms are highly sensitive to the concentrations of xanthine both in amplitude and waveform. At low concentration (400 μM), xanthine depletion is apparent from the tailing (transient) waveform, while at high xanthine concentrations (1600 μM), a classic sigmoidal wave is seen where the concentration of xanthine within the reaction layer is constant during the sweep. The sigmoidal voltammogram is indicative of an electrochemical steady state, i.e., the intermediate PMS_{ox} is consumed (by homogeneous reaction with XDH_{red}) at the same rate that it is generated at the electrode surface, and the forward and reverse sweeps are virtually identical.

For comparison, a series of voltammograms are shown in Figure 5 as a function of PMS concentration (2−4 μM) at a

dx.doi.org/10.1021/jp307374z | J. Phys. Chem. B 2012, 116, 11600−11607

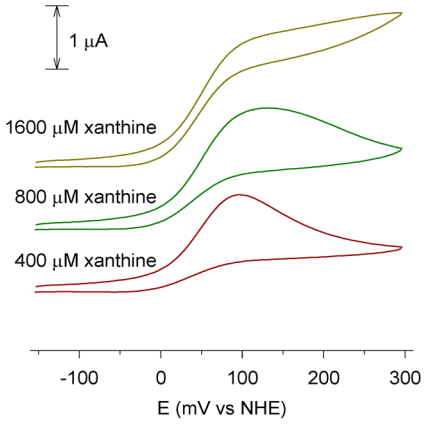

Figure 4. CVs obtained for PMS (5 μM) in the presence of 400, 800, and 1600 μM xanthine at the Au/HPyt/XDH electrode (50 mM Tris buffer, pH 8) at a sweep rate of 10 mV s^{-1}.

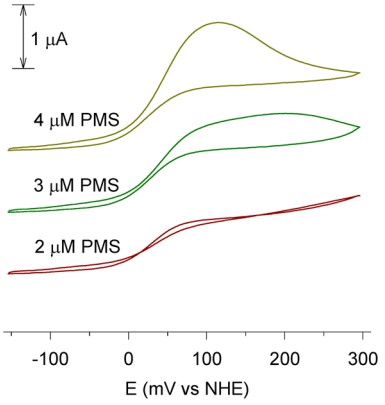

Figure 5. CVs obtained for PMS (2–4 μM) in the presence of 1000 μM xanthine at the Au/HPyt/XDH electrode (50 mM Tris buffer, pH 8) at a sweep rate of 5 mV s^{-1}.

fixed high xanthine concentration (1 mM) and sweep rate of 5 mV s^{-1}. At 2 μM PMS, a distinctly sigmoidal voltammogram is observed, indicative of an electrochemical steady state. At slightly higher PMS concentrations, the waveform becomes asymmetric due to depletion of xanthine within the reaction layer in an analogous manner to that seen in Figure 4. In other words the XDH:xanthine reaction (dependent on the concentration of PMS) is faster than mass transport of xanthine to the reaction layer at the electrode surface.

At higher sweep rates (10, 20, and 50 mV s^{-1}), the voltammetry becomes uniformly sigmoidal at all PMS concentrations in this range because diffusion layer expansion to give transient behavior is insignificant within the shorter time scale of the experiment (Supporting Information).

Hypoxanthine As Substrate. The same experiments were repeated with hypoxanthine as substrate at various concentrations of PMS and hypoxanthine. The XDH concentration, electrode surface area, and all other conditions were kept the same. Qualitatively, the results are very similar and show that the Au/HPyt/XDH electrode is also capable of catalyzing the oxidation of hypoxanthine. However, there are some notable differences (Figure 6). The experiments with hypoxanthine gave systematically higher catalytic currents (approximately twice as great) than comparable voltammetry with xanthine present (at the same XDH, PMS, and substrate concentrations).

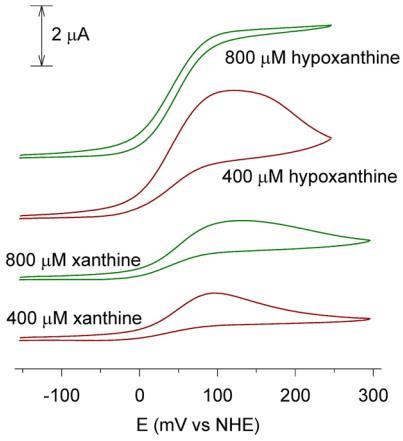

Figure 6. CVs obtained for PMS (5 μM) in the presence of 400 and 800 μM of hypoxanthine (top) and xanthine (bottom) at the Au/HPyt/XDH electrode (50 mM Tris buffer, pH 8) at a sweep rate of 10 mV s^{-1}.

Electrochemical Simulation. In previous work,[24,26] we have utilized voltammetry simulation to better understand the mechanism of mediated enzyme electrochemical reactions. Qualitatively, the overall reaction kinetics and voltammetric waveform (steady state or transient) are governed by the relative rates of the (second order) PMS_{ox}:XDH_{red} electron transfer cross-reaction, the XDH–xanthine reaction, which follows Michaelis–Menten kinetics (substrate dependent), and the heterogeneous electron transfer reaction of $PMS_{red/ox}$ (sweep rate dependent). As long as the sweep rates are not too high (in this case, <100 mV s^{-1}) the PMS_{ox}:XDH_{red} reaction is competitive, and the voltammetry approaches that of a steady state. If the bulk PMS concentration is too high, then the steady state breaks down (PMS_{ox} generated at the electrode overwhelms XDH_{red}), and the voltammetry is reminiscent of PMS alone (transient, reversible). Under the conditions of our experiments, the PMS concentration was kept low (2–5 μM) relative to the concentration of XDH under the membrane (ca. 3 mM). On this point, the initial concentration of XDH added to the electrode was 66 μM in a volume of ca. 3 μL. After attachment of the membrane, the XDH concentration increased by a factor of ~50 (ca. 3 mM) due to dialysis against the bulk solution and the very small internal volume between the membrane and the electrode (ca. 0.1 μL).

The objective of the simulation was to deduce rate constants defined in Scheme 2 that could reproduce all voltammetry performed at different sweep rates and concentrations of substrate and PMS. The voltammetric sweep rate is a powerful variable to elucidate the kinetics of electrochemical processes coupled with chemical reactions, and the DigiSim program[41] enables the same set of parameters to be optimized to CVs measured at a variety of sweep rates.[24,26] When the concentrations of PMS, XDH, or substrate are varied, then, ideally, the same parameters will reproduce the voltammetry.

XDH:Xanthine:PMS System. A single set of rate constants (Table 1) was obtained for the PMS:XDH:xanthine system that reproduced the experimental data over a wide range of xanthine and PMS concentrations and sweep rates from 2 to 50 mV s^{-1}. The XDH concentration was kept constant as much as possible given variations in the internal membrane volume. Some typical comparisons of experimental and simulated voltammetry at various sweep rates are shown in Figure 7. All simulations are given in the Supporting Information.

dx.doi.org/10.1021/jp307374z | J. Phys. Chem. B 2012, 116, 11600–11607

Table 1. Kinetic Parameters Derived from Electrochemical Simulation (Values in Italics Are Approximate)

	xanthine	hypoxanthine
k_1 (M^{-1} s^{-1})	1.8×10^5	1×10^5
k_{-1} (s^{-1})	4.5×10^3	1×10^3
k_2 (s^{-1})	100	60
k_{-2} (s^{-1})	*10*	*6.0×10^{-2}*
k_3 (s^{-1})	*100*	*100*
k_{-3} (M^{-1} s^{-1})	*8*	*1*
k_4 (M^{-1} s^{-1})	7.0×10^5	7.0×10^5
k_{-4} (M^{-1} s^{-1})	*70*	*70*
$K_{M,\ xanthine}$ (mM)	26	11

Hypoxanthine:XDH:PMS System. As mentioned above, it was surprising that the catalytic current effectively doubled moving from xanthine to hypoxanthine (Figure 6). Previous solution assays studies[20,42−44] of XDH and bovine XO have found that the specific activity toward xanthine is comparable with hypoxanthine. Given that the XDH concentrations were kept the same in each experiment and that the PMS concentrations were comparable, it is difficult to reconcile the increase (ca. 2-fold) in apparent activity of XDH toward hypoxanthine oxidation relative to xanthine.

In a recent article, we found that electrochemically driven turnover of XDH adsorbed on an edge plane pyrolytic graphite (EPG) electrode in reaction with hypoxanthine led, surprisingly, to the production of uric acid.[32] This behavior suggested two sequential 2-electron reactions (hypoxanthine to xanthine then xanthine to uric acid, Figure 1), but in a tightly coupled process where xanthine does not escape the reaction layer close to the electrode, but instead is rapidly recaptured by XDH for a second oxidation. Sequential hydroxylation of hypoxanthine has been observed in the exhaustive turnover of bovine XO with hypoxanthine.[44]

On the basis of the marked enhancement of catalytic current seen in these experiments, we are drawn to the same conclusion that the greatly enhanced catalytic currents seen for the PMS:XDH:hypoxanthine system relative to xanthine (Figure 6) are a due to a composite of both reactions (hypoxanthine → xanthine and xanthine → uric acid) occurring. To this end, the model was expanded to include xanthine as both the product of the first oxidation and substrate of the second oxidation (Scheme 3). The fits to the experimental data were again good, and the parameters for the XDH:hypoxanthine reactions are similar to those obtained for xanthine. Some representative CVs are shown in Figure 8 at both varying hypoxanthine concentration and PMS concentrations.

Mechanism. There is an important stereochemical consideration in the dual role played by xanthine in this mechanism (Scheme 3). Hydroxylation of hypoxanthine (at C2) results in the xanthinate anion coordinated to the Mo ion by its newly introduced O-atom. Xanthine *product* dissociates by ligand substitution (hydrolysis) of the Mo−O(xanthine) bond. The active site is reoxidized to Mo^{VI} by intramolecular electron transfer to the FAD cofactor and then reaction with PMS_{ox} in this case. The re-entering xanthine *substrate* must be oriented such that C8 is able to undergo attack by the equatorial hydroxido ligand on the Mo^{VI} active site, which is at the opposite end of the molecule from C2, the site of initial hypoxanthine hydroxylation (Scheme 3). Whether the *same* hypoxanthine molecule is able to undergo hydroxylation (to become xanthine), dissociate, rotate, and then undergo a second hydroxylation to produce uric acid within the confines of the active site is uncertain. Recent crystallographic work on bovine XO has shown that the active site may accommodate hypoxanthine in either orientation (with C8 or C2 adjacent to the Mo ion),[44] which indicates that the active site is large enough to accommodate a reorientation of the substrate, i.e., C2-oriented xanthine to C8-oriented xanthine. However, in an exhaustive enzymatic hydroxylation of hypoxanthine with XO, the intermediate xanthine accumulates during the experiment.[44] If two consecutive hydroxylation steps occurred on the same substrate, then xanthine would never be observed. This illustrated that xanthine dissociates into the bulk solution then reenters (in competition with hypoxanthine) for oxidation to uric acid under the conditions of that assay.

The situation here is subtly different. Voltammetry only involves reactions within the diffusion layer, which is only a millimeter or so from the electrode surface. So, unlike the exhaustive enzymatic hydroxylation experiments on bovine XO,[44] the bulk concentrations of hypoxanthine, xanthine, and uric acid do not change, and the voltammetry experiment is conducted over a much shorter time scale. For xanthine

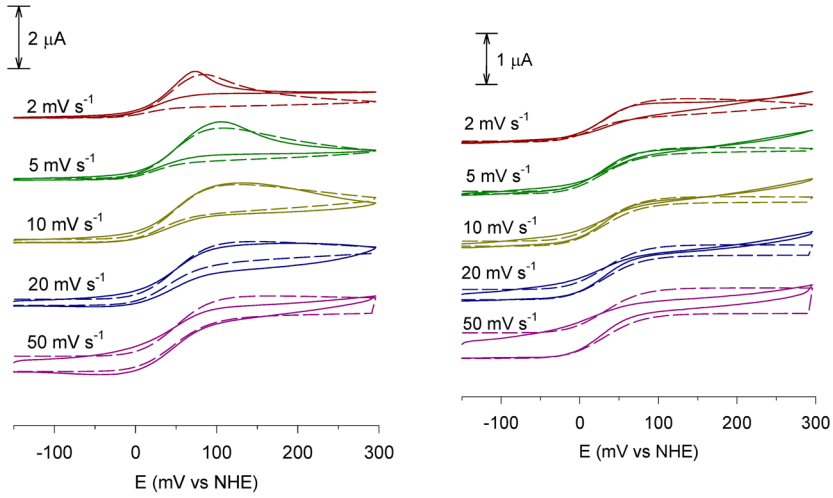

Figure 7. Experimental (solid lines) and simulated (broken lines) sweep rate dependent CVs obtained for (left) PMS (5 μM) in the presence of 800 μM of xanthine and (right) PMS (2 μM) in the presence of 1000 μM of xanthine at the Au/HPyt/XDH electrode (50 mM Tris buffer, pH 8).

dx.doi.org/10.1021/jp307374z | J. Phys. Chem. B 2012, 116, 11600−11607

Scheme 3

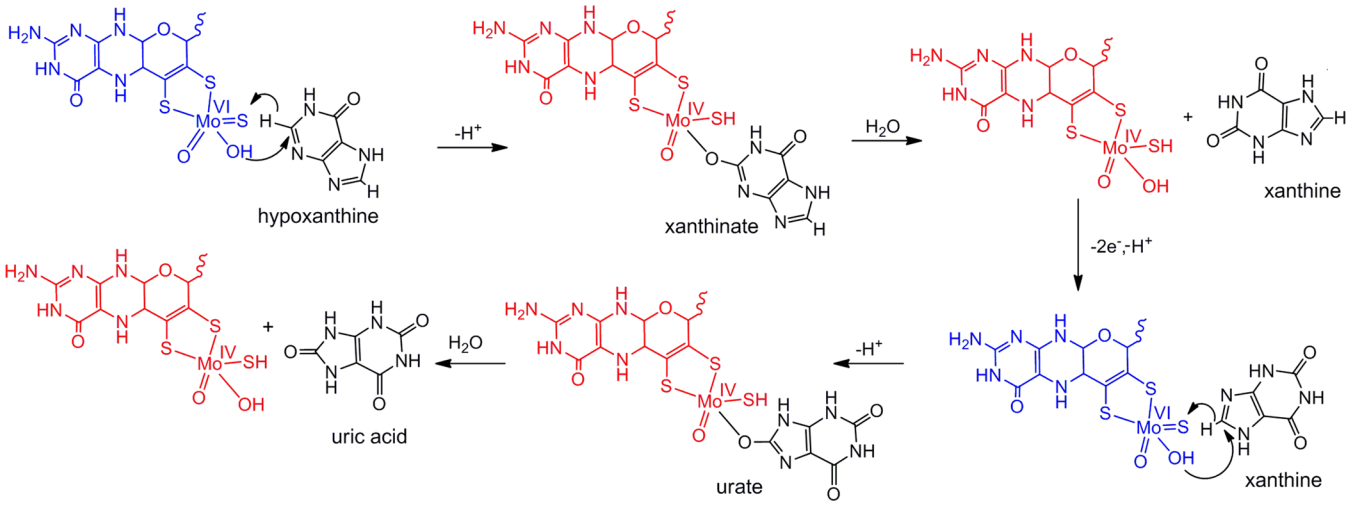

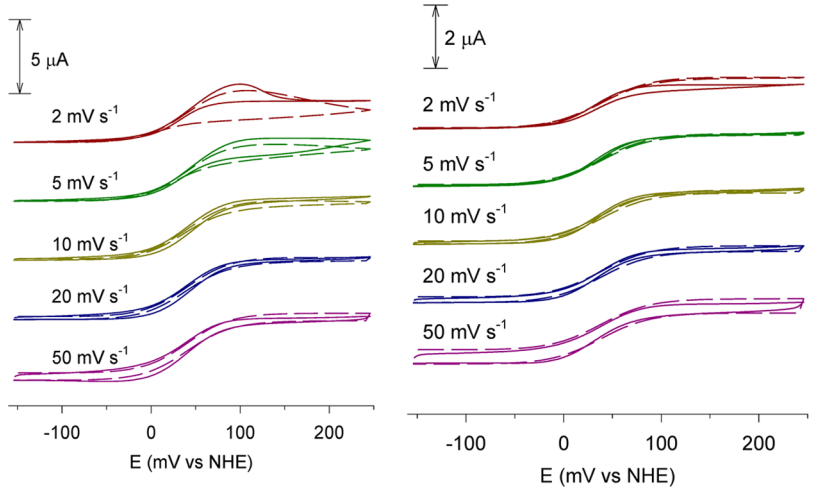

Figure 8. Experimental (solid lines) and simulated (broken lines) sweep rate dependent CVs obtained for (left) PMS (5 μM) in the presence of 800 μM of hypoxanthine and (right) PMS (3 μM) in the presence of 1000 μM of xanthine at the Au/HPyt/XDH electrode (50 mM Tris buffer, pH 8).

(produced by hypoxanthine hydroxylation) to be electroenzymatically reoxidized to uric acid, it must be recaptured by XDH rapidly before it escapes into the bulk solution where its concentration would be negligibly low. We propose that xanthine (product) dissociates from the XDH active site after the first hydroxylation but does not have time to diffuse away from the electrode surface before it is recaptured for a second hydroxylation, thus effectively doubling the catalytic current relative to the xanthine system. It is possible that the membrane covering the electrode impedes diffusion of xanthine from the reaction layer and facilitates the second oxidation step.

Analysis of Kinetics Parameters. A single set of rate and equilibrium constants defined in Scheme 2 reproduced all our experimental voltammetry undertaken at different sweep rates and various concentrations of xanthine and PMS (Table 1). The same PMS:XDH:xanthine parameters ($k_{4/-4}$, redox potential) were used in modeling the second hydroxylation step of the PMS:XDH:hypoxanthine reaction, which is identical in every way to the PMS:XDH:xanthine system. As with any simulation, the unique and accurate determination of multiple variables is problematic. Most steps were practically irreversible so the reverse rate constants (k_{-2}, k_{-3}, and k_{-4}) are only estimates, i.e., they are merely upper bounds. The rate of product release (k_3) was also not rate limiting under the conditions of the experiment. The turnover numbers for xanthine and hypoxanthine (k_2) are consistent with experimental values published for XDH in solution assays.[45] The outer sphere electron transfer rate constant k_4 is well-defined.

The apparent Michaelis constants for the substrate K_M $[(k_2+k_{-1})/k_1]$ are much larger than found in solution assays of XDH (30 μM).[20,44] The main cause for this is evidently a lower substrate binding rate constant (k_1). This parameter had a large influence on the quality of the fit. The reason that k_1 is lowered may be linked to inhibited access of the substrates to the active site of XDH within the confines of the thin layer under the membrane. Certainly, the continual increase in current as a function of already high substrate concentrations (>400 μM) seen in Figure 6 for both hypoxanthine and xanthine reflects a very high apparent K_M value (where saturation has still not been reached). This extended dynamic range is also indicative of substrate mass transport becoming rate limiting rather than enzyme kinetics. The passage of substrate across the membrane, in this case, is somewhat hampered and is responsible for the lack of substrate saturation even at concentrations well above the reported solution K_M value. So, the apparent K_M values calculated here should be

dx.doi.org/10.1021/jp307374z | J. Phys. Chem. B 2012, 116, 11600−11607

taken in context as being a consequence of the experiment rather than reflecting an intrinsic change to the properties of the enzyme.

CONCLUSIONS

The mediated electrocatalytic voltammetry of XDH in reaction with its substrates xanthine and hypoxanthine was investigated using PMS as an artificial mediator. This represents the first time that a xanthine oxidoreductase from any organism has been electrochemically investigated without interference from product (uric acid) interference or denaturation. The complexities of this enzyme have brought many challenges, but by careful selection of the redox potential of our mediator, we have been able to selectively activate the enzyme within a potential window where product oxidation does not occur. Both transient and sigmoidal voltammograms were obtained depending upon mediator and substrate concentration and sweep rate. Digital simulation enabled the kinetics of the enzymatic reaction to be understood as a function of the substrate and mediator concentration at different sweep rates, and a single set of rate constants was obtained that modeled the experimental data. In particular, the modeling reveals that the pronounced catalytic activity of hypoxanthine in reaction with XDH is due to a sequential (overall four electron) oxidation to uric acid involving the intermediate xanthine playing a dual role as first product then as substrate.

ASSOCIATED CONTENT

Supporting Information

Experimental and simulated voltammograms. This material is available free of charge via the Internet at http://pubs.acs.org.

AUTHOR INFORMATION

Corresponding Author

*E-mail: p.bernhardt@uq.edu.au.

Notes

The authors declare no competing financial interest.

ACKNOWLEDGMENTS

We gratefully acknowledge financial support from the Australian Research Council Discovery Grants DP0880288 & DP120101465 (to P.V.B.) and from the Deutsche Forschungsgemeinschaft Cluster of Excellence "Unifying concepts in catalysis" (to S.L.).

REFERENCES

(1) Bernhardt, P. V. *Aust. J. Chem.* **2006**, *59*, 233−256.
(2) Bernhardt, P. V. *Chem. Commun.* **2011**, *47*, 1663−1673.
(3) Yemini, M.; Reches, M.; Gazit, E.; Rishpon, J. *Anal. Chem.* **2005**, *77*, 5155−5159.
(4) Kausaite-Minkstimiene, A.; Mazeiko, V.; Ramanaviciene, A.; Ramanavicius, A. *Sens. Actuators, B* **2011**, *158*, 278−285.
(5) Sahin, A.; Dooley, K.; Cropek, D. M.; West, A. C.; Banta, S. *Sens. Actuators, B* **2011**, *158*, 353−360.
(6) Zhang, H.; Meng, Z.; Wang, Q.; Zheng, J. *Sens. Actuators, B* **2011**, *158*, 23−27.
(7) Somers, W.; Dool, R. T. M.; Jong, G. A. H.; Jongejan, J. A.; Duine, J. A.; Lugt, J. P. *Biotechnol. Tech.* **1994**, *8*, 407−412.
(8) Kang, Y.-W.; Kang, C.; Hong, J.-S.; Yun, S.-E. *Biotechnol. Lett.* **2001**, *23*, 599−604.
(9) Bourdillon, C.; Demaille, C.; Moiroux, J.; Saveant, J.-M. *Acc. Chem. Res.* **1996**, *29*, 529−535.
(10) Bourdillon, C.; Demaille, C.; Gueris, J.; Moiroux, J.; Saveant, J.-M. *J. Am. Chem. Soc.* **1993**, *115*, 12264−12269.
(11) Anicet, N.; Bourdillon, C.; Moiroux, J.; Saveant, J.-M. *J. Phys. Chem. B* **1998**, *102*, 9844−9849.
(12) Limoges, B.; Marchal, D.; Mavre, F.; Saveant, J.-M. *J. Am. Chem. Soc.* **2006**, *128*, 2084−2092.
(13) Bernhardt, P. V.; Chen, K.-I.; Sharpe, P. C. *J. Biol. Inorg. Chem.* **2006**, *11*, 930−936.
(14) Hille, R. *Chem. Rev.* **1996**, *96*, 2757−2816.
(15) Choi, E.-Y.; Stockert, A. L.; Leimkühler, S.; Hille, R. *J. Inorg. Biochem.* **2004**, *98*, 841−848.
(16) Enroth, C.; Eger, B. T.; Okamoto, K.; Nishino, T.; Nishino, T.; Pai, E. F. *Proc. Natl. Acad. Sci. U.S.A.* **2000**, *97*, 10723−10728.
(17) Borges, F.; Fernandes, E.; Roleira, F. *Curr. Med. Chem.* **2002**, *9*, 195−217.
(18) Leimkühler, S.; Kern, M.; Solomon, P. S.; McEwan, A. G.; Schwarz, G.; Mendel, R. R.; Klipp, W. *Mol. Microbiol.* **1998**, *27*, 853−869.
(19) Truglio, J. J.; Theis, K.; Leimkühler, S.; Rappa, R.; Rajagopalan, K. V.; Kisker, C. *Structure* **2002**, *10*, 115−125.
(20) Leimkühler, S.; Hodson, R.; George, G. N.; Rajagopalan, K. V. *J. Biol. Chem.* **2003**, *278*, 20802−20811.
(21) Mao, L.; Xu, F.; Xu, Q.; Jin, L. *Anal. Biochem.* **2001**, *292*, 94−101.
(22) Nishino, T.; Nishino, T.; Schopfer, L. M.; Massey, V. *J. Biol. Chem.* **1989**, *264*, 2518−27.
(23) Creevey, N. L.; McEwan, A. G.; Bernhardt, P. V. *J. Biol. Inorg. Chem.* **2008**, *13*, 1231−1238.
(24) Chen, K.-I.; McEwan, A.; Bernhardt, P. *J. Biol. Inorg. Chem.* **2009**, *14*, 409−419.
(25) Kalimuthu, P.; Tkac, J.; Kappler, U.; Davis, J. J.; Bernhardt, P. V. *Anal. Chem.* **2011**, *82*, 7374−7379.
(26) Chen, K.-I.; McEwan, A. G.; Bernhardt, P. V. *J. Biol. Inorg. Chem.* **2011**, *16*, 227−234.
(27) Aguey-Zinsou, K.-F.; Bernhardt, P. V.; Kappler, U.; McEwan, A. G. *J. Am. Chem. Soc.* **2003**, *125*, 530−535.
(28) Bernhardt, P. V.; Santini, J. M. *Biochemistry* **2006**, *45*, 2804−2809.
(29) Rapson, T. D.; Kappler, U.; Bernhardt, P. V. *Biochim. Biophys. Acta, Bioenerg.* **2008**, *1777*, 1319−1325.
(30) Rapson, T. D.; Kappler, U.; Hanson, G. R.; Bernhardt, P. V. *Biochim. Biophys. Acta, Bioenerg.* **2011**, *1807*, 108−118.
(31) Aguey-Zinsou, K. F.; Bernhardt, P. V.; Leimkühler, S. *J. Am. Chem. Soc.* **2003**, *125*, 15352−15358.
(32) Kalimuthu, P.; Leimkühler, S.; Bernhardt, P. V. *J. Phys. Chem. B* **2011**, *115*, 2655−2662.
(33) Bernhardt, P. V.; Honeychurch, M. J.; McEwan, A. G. *Electrochem. Commun.* **2006**, *8*, 257−261.
(34) Hason, S.; Stepankova, S.; Kourilova, A.; Vetterl, V.; Lata, J.; Fojta, M.; Jelen, F. *Anal. Chem.* **2009**, *81*, 4302−4307.
(35) Hansen, B. H.; Dryhurst, G. *J. Electroanal. Chem. Interfacial Electrochem.* **1971**, *30*, 417−426.
(36) Dryhurst, G. *Bioelectrochem. Bioenerg.* **1974**, *1*, 49−66.
(37) Luong, J. H. T.; Thatipamala, R. *Anal. Chim. Acta* **1996**, *319*, 325−333.
(38) Liu, Y.; Nie, L.; Tao, W.; Yao, S. *Electroanalysis* **2004**, *16*, 1271−1278.
(39) Tkac, J.; Davis, J. J. *J. Electroanal. Chem.* **2008**, *621*, 117−120.
(40) Paulo, T. d. F.; da Silva, M. A. S.; Pinheiro, S. d. O.; Meyer, E.; Pinheiro, L. S.; Freire, J. A.; Tanaka, A. A.; de Lima Neto, P.; Moreira, Í. d. S.; Diógenes, I. C. N. *J. Braz. Chem. Soc.* **2008**, *19*, 711−719.
(41) Rudolf, M.; Feldberg, S. W. *DigiSim*, 3.03b; Bioanalytical Systems: West Lafayette, IN, 2004.
(42) Leimkühler, S.; Stockert, A. L.; Igarashi, K.; Nishino, T.; Hille, R. *J. Biol. Chem.* **2004**, *279*, 40437−40444.
(43) Pauff, J. M.; Hemann, C. F.; Juenemann, N.; Leimkühler, S.; Hille, R. *J. Biol. Chem.* **2007**, *282*, 12785−12790.
(44) Cao, H.; Pauff, J. M.; Hille, R. *J. Biol. Chem.* **2010**, *285*, 28044−28053.

(45) Schumann, S.; Saggu, M.; Moeller, N.; Anker, S. D.; Lendzian, F.; Hildebrandt, P.; Leimkühler, S. *J. Biol. Chem.* **2008**, *283*, 16602−16611.